Int. J. Heat Mass Transfer. Vol. 26, No. 3, pp. 471–474, 1983
Printed in Great Britain

0017-9310/83/030471-04 $03.00/0

TECHNICAL NOTES

COMBINED FREE AND FORCED CONVECTION BETWEEN HORIZONTAL PARALLEL PLANES: SOME CASE STUDIES

K. J. KENNEDY
Bell Telephone Laboratories, Holmdel, NJ 07733, U.S.A.

and

A. ZEBIB
Department of Mechanical Engineering, Rutgers University, New Brunswick, NJ 08903, U.S.A.

NOMENCLATURE

α, local heat transfer coefficient;
b, channel height;
L, channel length;
λ, thermal conductivity;
ν, kinematic viscosity;
Pr, Prandtl number;
q, heat flux;
T_r, reference temperature, qb/λ;
T_∞, inlet temperature;
U_∞, inlet velocity;
x, axial coordinate;
y, vertical coordinate;
γ, isobaric compressibility.

Dimensionless variables
Gr, Grashof number, $g\gamma T_r b^3/\nu^2$;
Nu, Nusselt number, $2b\alpha/\lambda$;
Re, Reynold's number, $2bU_\infty/\nu$;
θ, temperature, $(T-T_\infty)/T_r$.

INTRODUCTION

COMBINED free and forced convection cooling in horizontal channels is of interest to heat exchanger and electronic packaging designers. The latter application, cooling microelectronic circuitry, motivated this study. A typical large scale integrated circuit (IC) can dissipate as much as 2 W in a 7.5 cm^2 package. Heat is conducted through the leads of the IC to the printed wiring board or directly convected to the air. These high local power densities and horizontal printed wiring board configurations have required forced convection cooling of the circuitry. The traditional assumption of uniform heat flux printed wiring boards is no longer warranted [1].

An analytical investigation by Gill and Del Casal [2] studied the effect of buoyancy on fully developed laminar flow between parallel planes. Their analysis can be extended to determine Nusselt numbers for both walls heated at the same rate. In this case, a separated recirculating flow occurs at the upper wall. The fully developed Nusselt numbers on the upper and lower walls can be calculated to be 5.14 and 11.98, respectively. A numerical study by Nguyen, Maclaine-cross and de Vahl Davis [3] assessed the impact of entrance effects in a forced horizontal parallel plane flow due to buoyancy. The walls were isothermal and the Reynolds numbers were low, such that the flow was 2-dim. The numerical solution was obtained by the method of false transient. Their results evidence a small separation region on the upper wall. Heat transfer above a heated plate was enhanced while decreased below a heated plate with respect to *purely* forced flows.

Kamotani, Ostrach and Miao [4] experimentally studied the effects of thermal instability on heat transfer on developing horizontal forced flow between parallel planes. They showed that thermal instability could increase the heat transfer rate by a factor of 4 along the lower wall in the entrance region.

Kennedy and Zebib [5] presented numerical and experimental results on the effects of free convection on a forced laminar horizontal channel flow with a local heat source on the lower wall. In this case, ($Re = 37$ and $Gr = 5.4 \times 10^5$) the effect of free convection was to form a recirculation region adjacent to the top wall, above the heat source. A dramatic jump in the fluid passing over the source at the lower wall was observed downstream of the source. Buoyancy enhanced the heat transfer rate on the source by a factor of two as compared with the solution without buoyancy.

In this technical note, attention is focused on the heat transfer characteristics and flow patterns resulting from four specific local heat source configurations. These cases are used to formulate design guidelines. A discussion of the difficulties encountered in the numerical investigation is provided.

NUMERICAL SOLUTION

Figure 1 depicts a 2-dim. channel of length, L and height b. The walls are insulated everywhere except at a distance (X_h) from the inlet where a heat source of length (L_s), and magnitude (Q) is located. An arbitrary heat flux distribution can then be described by dividing the planes into a finite number of local sources with some uniform flux on each source. The uniform inlet velocity profiles are denoted by U_∞ and T_∞, respectively. The origin of the coordinate system is located in the lower left hand corner.

Three dimensionless parameters discussed in this paper, Grashof number, Nusselt number, and Reynolds number are defined in terms of the following quantities: local heat transfer coefficient (α), thermal conductivity (λ), kinematic viscosity (ν), isobaric compressibility (γ), heat flux per unit area (q), gravitational constant (g), and reference temperature T_r. The Grashof number (Gr) is given by $Gr = g\gamma T_r b^3/\nu^2$, where $T_r = qb/\lambda$. The Nusselt number (Nu) and Reynold's number (Re) are defined by the quantities, $2b\alpha/\lambda$ and $2bU_\infty/\nu$, respectively.

The original plan of this investigation was to develop a parabolic numerical solution in regions of small axial gradients. This solution would be patched to an elliptic solution in regions of large axial gradients. A stable parabolic solution for the mixed convection problem was not found although several methods were attempted by Kennedy [6]. These methods included extensions of the method of Hornbeck and Carlson [7] and Keller's box scheme [8]. In the first method, instability was observed as the vertical nodes were increased beyond 15. The limitation on the axial step size [7] was also observed. As the vertical step size decreased, the coefficient of the pressure terms increased, resulting in an ill-

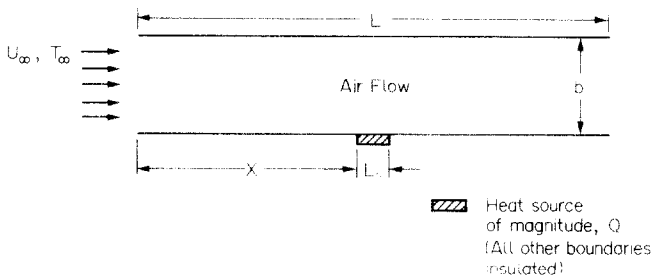

FIG. 1. Configuration of channel flow.

conditioned matrix inversion. This same method, with the buoyancy and vertical pressure gradient removed from the formulation resulted in a stable solution. The vorticity formulation, in conjunction with Keller's box scheme, was also found to be unstable.

Because a successful parabolic method was not obtained, an elliptic scheme, the method of false transient [9], was used for the entire duct. This method parabolizes the Poisson equation by adding a false time derivative. Different transient coefficients, α_ω, α_ψ and α_Θ are introduced into the governing equations to accelerate convergence. These coefficients are determined through numerical experimentation. A mapping function, $\eta(x)$, is also employed to provide the necessary grid resolution in regions near the heat source where large axial gradients are expected. The details of this implementation can be found elsewhere [5, 6].

EXPERIMENTAL APPARATUS

The experimental apparatus has been described elsewhere [5, 6]. Only a summary is provided here. The 66 cm long Plexiglas channel was constructed. The height and depth of the channel were 1.325 cm and 17.8 cm, respectively. Air was drawn through the duct.

The heating element consisted of two identical printed wiring boards, assembled in tandem, approximately 5 mm apart. The lower board acted as a guard heater for the upper board. Each epoxy glass printed wiring board was 1.6 mm thick. The heat source was made by adding a 0.032 mm thickness of copper using an electroless copper deposition process. A layer of gold (30 μm thick) was electrodeposited onto the copper. The use of gold on the heat source resulted in a low emissivity surface, $\varepsilon = 0.05$.

The experimental uncertainty of the flowrate for the cases of $Re = 37$ presented is about 15% [6]. Radiation losses were estimated to be about 10% for these cases.

DISCUSSION

Figure 2 compares experimental and numerical results for a Reynold's number of 790, emissivity of zero, duct height of 1.325 cm, and a heat source length of 15.24 cm. Temperature profiles are depicted as a function of the buoyancy coefficient, K, defined as $K = 4Gr/Re^2$. The parabolic numerical code used for this verification has been presented [6] and shown to be in good agreement with the results of Naito [10]. This code uses the familiar finite difference schemes of Carlson and Hornbeck [7] without the vertical pressure gradient and buoyancy terms. Therefore, for small values of K and low wall temperatures, excellent agreement is evidenced for K equal to 0.06 and 0.156. An increase in heat flux (larger K) created greater discrepancies in the results. Longitudinal vortex rolls were observed about 5 cm downstream of the heater end for $K \geqslant 0.28$. Flow visualization also evidenced a spread of the fluid over the plate as it approached the point where the jump and vortex rolls began. This phenomena is lucidly described by Kamotani, Ostrach and Miao [4].

The heat source locations for each of the four cases discussed are:

Case 1. 6 mm heat source on lower wall;
Case 2. 18 mm heat source on lower wall;
Case 3. 6 mm heat source on upper wall;
Case 4. 6 mm heat source on both walls.

The first case was discussed in detail in ref. [5] and is

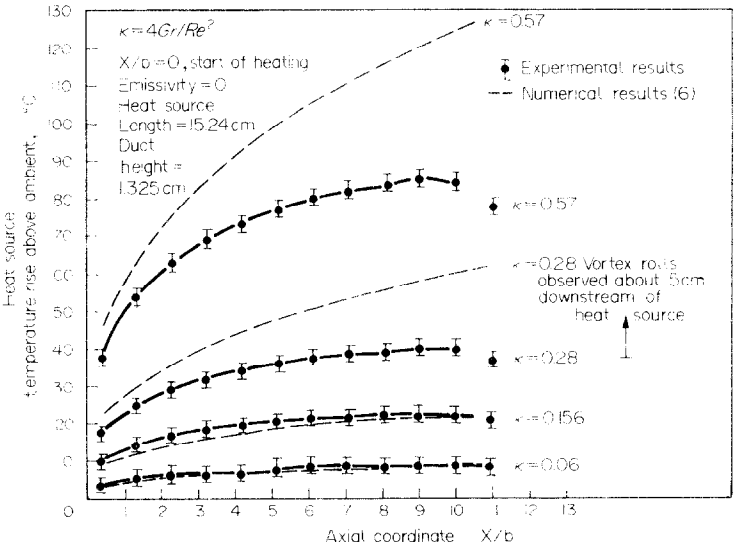

FIG. 2. Comparison between experimental and numerical heat source temperature profiles: $Re = 790$.

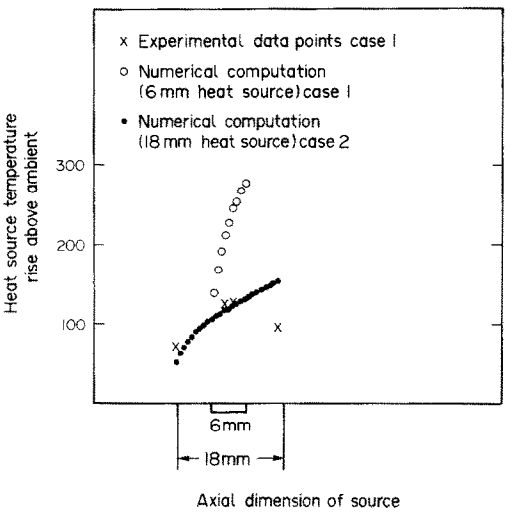

FIG. 3. Comparison of numerical and experimental temperature profiles.

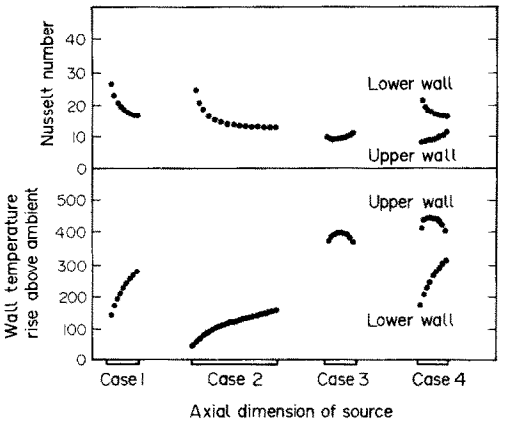

FIG. 4. Comparison of heat transfer characteristics of four local source configurations.

mentioned here for the purpose of comparison. All of the heat sources in cases 1–4 were centrally located at 7.65 duct heights from the channel entrance. In cases 1, 3 and 4 the heat sources were 6 mm long. Case 2 studies an 18 mm long heat source. A Reynold's number of 37 is studied in each case. The overall heat input (W) at any one source, denoted by Q, is the same. The Grashof number in each case is as follows: Cases 1, 3, 4, $Gr = 5.4 \times 10^5$; and Case 2, $Gr = 1.8 \times 10^5$.

Figure 3 compares the experimental and numerical temperature profiles of case 1, with the numerical result of case 2. It had been reported that axial conduction contributed at least 30% of the heat loss off the source in case 1 [5]. Since thermocouple measurements were available over an 18 mm length in case 1, it seemed reasonable to consider case 2 numerically, where the same overall power input of case 1 was dissipated in three times the original area. It can be seen that the numerical results of case 2 more closely describe the experimental temperature rise than do the numerical results of case 1. Although it is not suggested that case 2 is an accurate description of the heat transfer, it is supporting evidence for the large axial conduction loss. Axial conduction not only decreases the magnitude of the temperature profile but alters the shape as evidenced by the temperature drop observed experimentally, downstream of the heater. Moreover, the recirculation region above the source reported in ref. [5] grew slightly, i.e. though the Grashof number in case 2 was one-third that of case 1, the same flow configuration resulted.

Figure 4 depicts a comparison of the local Nusselt numbers and wall temperature profiles on the heat sources. The lowest wall temperatures are evidenced in case 2 where the power dissipation is on the lower wall and the heat transfer area is largest. A comparison of cases 1 and 3 indicates the lowest wall temperature for the 6 mm heat source is obtained with the source at the bottom wall. The Nusselt numbers in case 1 are approximately twice those of case 3. Figure 5(a) is a stream function plot for case 3. The recirculation region of case 3 is observed to be moved slightly upstream of the source and the result of case 1. The relative maximums of the temperature profiles for heat sources located on the upper wall are explained by the stagnation points occurring there. At these locations the local velocities are smallest, resulting in maximum temperatures.

A comparison of the wall temperatures of cases 1 and 3 to the corresponding temperatures in case 4 evidences an increase of more than 10% in the wall temperatures. The complex flow pattern of case 4 is illustrated in Fig. 5(b).

These results suggest several guidelines for the thermal design of electronic packages. When dealing with high power densities in forced horizontal channel flow, the greatest power dissipators should be placed along the lower wall. A device placed on the top wall will realize temperatures almost twice those had the device been located on the lower wall. Physically, this behavior occurs because heating on the lower wall greatly accelerates the adjacent fluid and enhances heat transfer. Along the upper wall, heating retards the fluid and results in higher temperatures. Interaction between devices placed

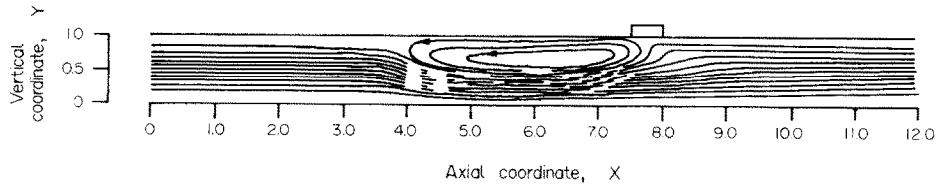

FIG. 5(a). Streamfunction plots for 6 mm heat source: $Re = 37$, case 3.

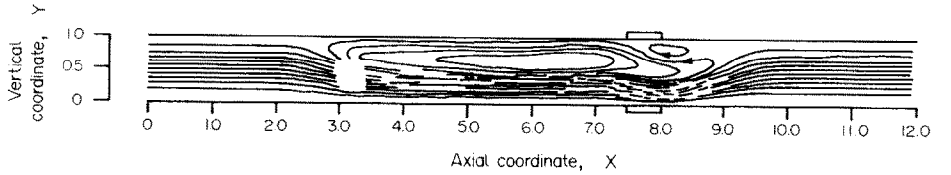

FIG. 5(b). Streamfunction plots for 6 mm heat source: $Re = 37$, case 4.

directly above one another can be significant. In the case mentioned above, the temperatures increased by more than 10% with respect to the case of no interaction, i.e. one device only.

The numerical results of cases 3 and 4 were obtained with a mapping function for which ΔX_{min} and C were equal to 0.05 and 1.125, respectively, as defined in ref. [5]. An 84 × 21 grid was employed such that nodes 31 through 39 represented the heat source. Minimum ΔX spacings where fixed between nodes 25 and 45. These numerical results were obtained with the following transient coefficients and time step: $\alpha_\omega = 0.01$, $\alpha_\psi = 1.0$, $\alpha_\Theta = 1.0$ and $\Delta\tau = 0.02$. The computations required about 1.2 CPU hours on Bell Laboratories IBM 370/168 computer. These results were obtained with significantly less computing time than the results of case 1 (2 CPU hours) [5]. Although a larger number of nodes were used in the present study, the new mapping function resulted in a smaller overall duct length. The time step used for the new results was twice that used in ref. [5]. Earlier experimentation with this code showed that heat flux boundary specification significantly increased the necessary computing times, as compared with constant wall temperature boundary conditions. The overall duct length was also observed to play a pronounced role in determining the time for convergence.

For future work, the strong effect of axial conduction found experimentally in these local source problems requires the rigorous addition of axial conduction into the numerical solution. Another problem of interest would be to study the effects on heat transfer of a strong heat source upstream of an equivalent or weaker source along the same wall, and the resulting wake interaction.

REFERENCES

1. A. E. Zinnes, An investigation of steady two dimensional laminar natural convection from a vertical plate of finite thickness with plane localized heat sources on its surface. Ph.D. Dissertation, Lehigh University, Bethlehem, PA (1969).
2. W. N. Gill and E. Del Casal, A theoretical investigation of natural convection effects in forced horizontal flows, *A.I.Ch.E. Jl* **8**, 513–581 (1962).
3. T. V. Nguyen, I. L. Maclaine-cross and G. de Vahl Davis, *Combined Forced and Free Convection Between Parallel Plates*, in *Numerical Methods in Thermal Problems*, pp. 269–278. Pine Ridge Press, U.K. (1979).
4. Y. Kamotani, S. Ostrach and H. Miao, Convective heat transfer augmentation in thermal entrance regions by means of thermal instability, *J. Heat Transfer* **101**, 222–233 (1979).
5. K. J. Kennedy and A. Zebib, Combined forced and free convection between parallel plates, Paper 82-IHTC-152. *Proc. 7th Int. Heat Transfer Conf.* Hemisphere, New York (1982).
6. K. J. Kennedy, An investigation of combined free and forced convection for laminar horizontal channel flow with local heat sources prescribed on the boundaries, Ph.D. Dissertation, Rutgers University, New Brunswick, New Jersey (1982).
7. G. A. Carlson and R. W. Hornbeck, A numerical solution for laminar entrance flow in a square duct, *J. Appl. Mech.* March (1973).
8. H. B. Keller, A new difference scheme for parabolic problems, in *Numerical Solutions of P.D.E.*, Vol. II, pp. 327–350. Academic Press, New York (1973).
9. G. D. Mallinson and G. de Vahl Davis, The method of false transient for the solution of coupled elliptic equations, *J. Comp. Phys.* **12**, 435–461 (1973).
10. E. Naito, Laminar heat transfer in the entrance region of parallel plates: The case of uniform heat flux, *Int. J. Chem. Engng* **16**, 162–170 (1976).

Int. J. Heat Mass Transfer. Vol. 26, No. 3, pp. 474–477, 1983
Printed in Great Britain

0017-9310/83/030474-04 $03.00/0

FREQUENCY DEPENDENCE IN THE EQUIVALENT DIFFUSIVITY

ROBERT KUKLINSKI* and BENN GOLD
Dept. of Mathematical Sciences, Worcester Polytechnic Institute, Worcester, MA 01609, U.S.A.

(*Received* 2 *October* 1981 *and in revised form* 8 *July* 1982)

NOMENCLATURE

Greek symbols

- ω, frequency of harmonic excitation;
- λ, eigenvalue in Fourier method;
- ν, dimensionless frequency parameter;
- ξ, eigenvalue;
- κ, (equivalent) diffusivity;
- α, coefficients in low frequency series expansion of ξ.

Subscripts

- M, refers to matrix layer;
- F, refers to filler layer;
- eq, refers to equivalent property.

1. INTRODUCTION

THE PROBLEM of determining the temperature distribution in bilaminates which are stacked parallel to an harmonically excited heat flow of frequency ω (Fig. 1), using effective thermal properties, has drawn considerable attention in recent years. In the case of a steady exciting heat source, it is well known that a single parameter, the equivalent diffusivity η_{eq}, will characterize the heat flow. Even for composites of materials with similar properties, the equivalent diffusivity will be adequate for the non-steady source of any low frequency. On the other hand, if ω is not vanishingly small, or if the materials differ greatly, then it has been suggested [5] that η_{eq} should be replaced by two equivalent diffusivities, η_P and η_A, diffusivity for phase and amplitude respectively, each dependent on the frequency. An experimental study by Truong and Zinsmeister [6] confirmed the failure of the static equivalent diffusivity and demonstrated that, in the cases they considered, η_P was roughly equal to η_{eq}, whereas η_A was less than η_{eq}. These results were the more obvious in composites of very unlike material. Difficulties inherent in determining experimental values of η_A and η_P at high exciting frequencies highlight the importance of an analytic solution of the heat equation that will yield explicit values for η_A and η_P.

We present an analytic attack of the problem of determining these effective thermal constants. We find it more convenient to use a dimensionless frequency parameter ν. Expanding the work of Horvay [5] to develop a frequency dependent η_{eq} allows explicit results for η_A and η_P. Numerical refinements of η_{eq} using Pade approximants and Newton's method, as well as

* Present address: Sun-Life of Canada, Wellesley, Mass. U.S.A.